

important role of molecular orientation. Though beyond the scope of the qualitative analysis presented here, changing the charge state of a molecule can markedly alter the orientational forces it experiences in its interaction with the metal surface. Thus, bond reorientation of the NO molecule may play a crucial role in the vibrational autodesorption mechanism. Such work should help to elucidate the nonadiabatic dynamics involved in dissociation, recombination, and reactions of molecules on metal surfaces.

References and Notes

- M. Born, J. R. Oppenheimer, *Ann. Phys.* **84**, 457 (1927).
- W. Kohn, L. J. Sham, *Phys. Rev.* **140**, A1133 (1965).
- J. Greeley, J. K. Norskov, M. Mavrikakis, *Annu. Rev. Phys. Chem.* **53**, 319 (2002).
- K. M. Neyman, F. Illas, *Catal. Today* **105**, 2 (2005).
- T. Greber, *Surf. Sci. Rep.* **28**, 1 (1997).
- H. Nienhaus, *Surf. Sci. Rep.* **45**, 1 (2002).
- C. T. Rettner, F. Fabre, J. Kimman, D. J. Auerbach, *Phys. Rev. Lett.* **55**, 1904 (1985).
- Y. Huang, C. T. Rettner, D. J. Auerbach, A. M. Wodtke, *Science* **290**, 111 (2000).
- Y. Huang, A. M. Wodtke, H. Hou, C. T. Rettner, D. J. Auerbach, *Phys. Rev. Lett.* **84**, 2985 (2000).
- A. M. Wodtke, J. C. Tully, D. J. Auerbach, *Int. Rev. Phys. Chem.* **23**, 513 (2004).
- Q. Ran, D. Matsiev, D. J. Auerbach, A. M. Wodtke, *Phys. Rev. Lett.* **98**, 237601 (2007).
- B. Gergen, H. Nienhaus, W. H. Weinberg, E. W. McFarland, *Science* **294**, 2521 (2001).
- X. Ji, A. Zupperro, J. M. Gidwani, G. A. Somorjai, *J. Am. Chem. Soc.* **127**, 5792 (2005).
- E. Hasselbrink, *Curr. Opin. Solid State Mater. Sci.* **10**, 192 (2006).
- D. J. Auerbach, *Science* **294**, 2488 (2001).
- J. D. White, J. Chen, D. Matsiev, D. J. Auerbach, A. M. Wodtke, *Nature* **433**, 503 (2005).
- J. D. White, J. Chen, D. Matsiev, D. J. Auerbach, A. M. Wodtke, *J. Chem. Phys.* **124**, 064702 (2006).
- Here, one ML is defined as one-to-one stoichiometric equivalence of Cs to surface Au atoms.
- T. Greber *et al.*, *Phys. Rev. B* **50**, 8755 (1994).
- E. E. Nikitin, *Annu. Rev. Phys. Chem.* **50**, 1 (1999).
- J. L. LaRue *et al.*, *J. Chem. Phys.* **129**, 024709 (2008).
- Under our conditions, the work function does not change over this time scale.
- R. T. Jongma, T. Rasing, G. Meijer, *J. Chem. Phys.* **102**, 1925 (1995).
- R. Brako, D. M. Newns, *Rep. Prog. Phys.* **52**, 655 (1989).
- L. Hellberg, J. Strömquist, B. Kasemo, B. I. Lundqvist, *Phys. Rev. Lett.* **74**, 4742 (1995).
- G. Katz, Y. Zeiri, R. Kosloff, *J. Phys. Chem. B* **109**, 18876 (2005).
- The quantum yield reported here is larger than previously reported in (16) and (17) due to detector saturation problems in the previous experiment.
- The energetics for electron transfer to the surface become only more favorable as the molecule approaches the surface.
- One may estimate tunneling distances based on principles set forth in (31).
- Energetically, the electron can originate from as much as 0.6 eV below the Fermi level, but this does not meaningfully alter the analysis presented here.
- N. Shenvi, S. Roy, P. Parandekar, J. Tully, *J. Chem. Phys.* **125**, 154703 (2006).
- Equation 1 is valid only in the limit of negligible depletion of the initial NO($V = 18$) population and thus small quantum yield. In the more general case, we must solve the differential equation for the population of NO($V = 18$). Equation 1 is then the first term of a Taylor series expansion of the solution.
- We gratefully acknowledge financial support from the NSF (grant CHE-0454806) and the Partnership for International Research and Education—for Electron Chemistry and Catalysis at Interfaces (NSF grant OISE-0530268). N.H.N. acknowledges financial support through a Feodor-Lynen fellowship provided by the Alexander von Humboldt Foundation. We thank D. Matsiev for many useful discussions and suggestions and a critical reading of this manuscript.

Supporting Online Material

www.sciencemag.org/cgi/content/full/321/5893/1191/DC1
SOM Text
References

5 May 2008; accepted 15 July 2008
10.1126/science.1160040

Weak Interplate Coupling by Seamounts and Repeating $M \sim 7$ Earthquakes

Kimihiro Mochizuki,^{1*} Tomoaki Yamada,¹ Masanao Shinohara,¹ Yoshiko Yamanaka,² Toshihiko Kanazawa¹

Subducting seamounts are thought to increase the normal stress between subducting and overriding plates. However, recent seismic surveys and laboratory experiments suggest that interplate coupling is weak. A seismic survey in the Japan Trench shows that a large seamount is being subducted near a region of repeating earthquakes of magnitude $M \sim 7$. Both observed seismicity and the pattern of rupture propagation during the 1982 $M 7.0$ event imply that interplate coupling was weak over the seamount. A large rupture area with small slip occurred in front of the seamount. Its northern bound could be determined by a trace of multiple subducted seamounts. Whereas a subducted seamount itself may not define the rupture area, its width may be influenced by that of the seamount.

Bathymetric relief on the ocean floor has been presumed to lead to variations in mechanical coupling along the plate interface between the overriding and subducting plates in the subduction zones, which in turn yield an uneven distribution of large earthquakes (1, 2). Seamounts, an obvious feature of topographic highs on subducting crust, having relative heights of more than 3000 m are not

uncommon (3). Such large seamounts may increase the normal stress between subducting and overriding plates by as much as 100 MPa when subducted (4), and it has been proposed that the raised interplate coupling could generate $M > 7$ earthquakes (2). Strong coupling over subducted seamounts has been proposed to explain rupture regions of large earthquakes in the Costa Rica subduction zone (5, 6) and a seismic barrier during the 1946 $M 8.1$ Nankaido earthquake (7).

Recent seismic surveys (8, 9) have shown that the base of the overriding plate is eroded while the decollement is shifted upward along with the subduction of a seamount, which would entrain fluid-rich sediment. Such effects, also seen in laboratory sandbox experiments (10), are ex-

pected to induce local weak interplate coupling; the damage caused by erosion may prevent the accumulation of elastic strain energy (11), and elevated pore pressure may reduce the effective normal stress (12). Local weak coupling at the plate interface is in accord with seismic surveys showing that some subducted seamounts have retained their shapes to depths of at least ~ 8 km (8, 9). Here, we examine a long-term record of seismicity in the Japan Trench to clarify the relation between seamounts and large earthquakes.

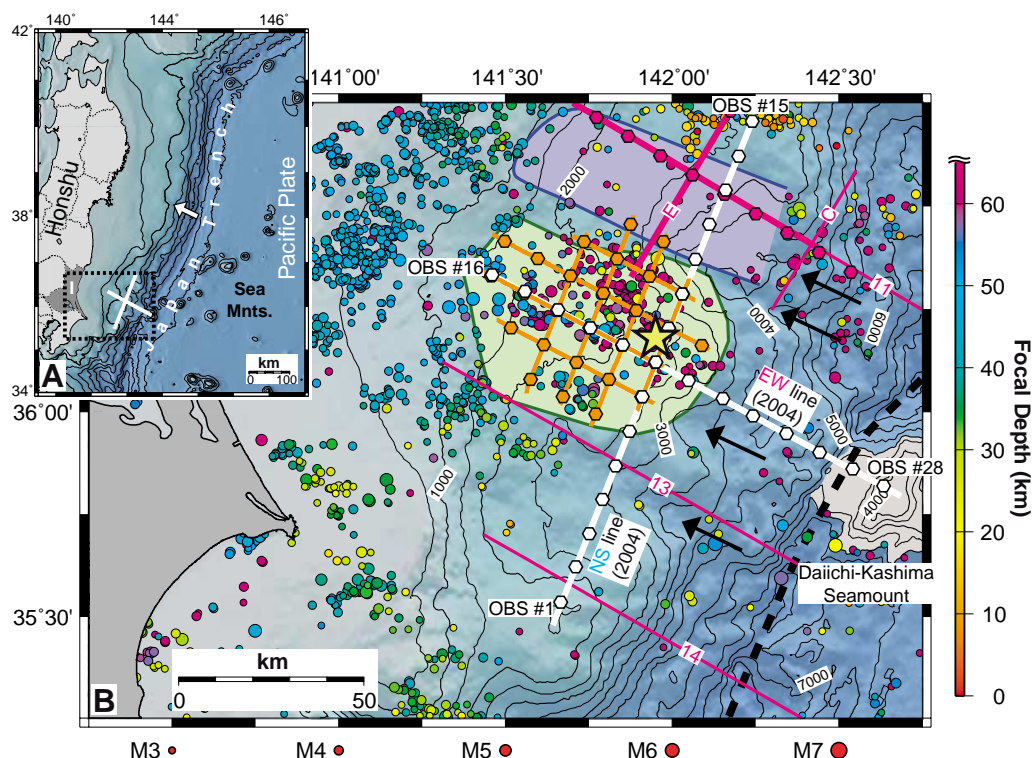
The Pacific Plate subducts beneath the North American Plate at ~ 8.3 cm/year along an azimuth of 295° along the Japan Trench (13) and contains a group of seamounts of various dimensions (Fig. 1), including Daiichi-Kashima Seamount, which entered the trench 150,000 to 250,000 years ago (14). Volcanic rock samples collected from the seamount yield an age of 100 to 120 million years, ~ 20 million years younger than the surrounding oceanic crust (14). Several furrows on the landward slope of the seafloor correlate with the distribution of seamounts on the offshore Pacific Plate (Fig. 1). Sandbox experiments reproduce such furrows oriented in the subduction direction behind subducting seamounts (10, 15). Similar furrows are seen along the Middle America Trench off Costa Rica (5, 8, 15). Repeating large earthquakes with a fairly constant size ($M \sim 7$) and a recurrence interval (~ 20 years) have occurred in a confined region down-dip from the Daiichi-Kashima Seamount since the 1920s (Fig. 2). Such occurrences suggest the existence of a stationary area of repeating rupture along the plate interface.

The most recent large event occurred in 1982 (another $M \sim 7$ earthquake likely along the series

¹Earthquake Research Institute, University of Tokyo, 1-1-1, Yayoi, Bunkyo-ku, Tokyo 113-0032, Japan. ²Graduate School of Environmental Studies, Nagoya University, Furo-cho, Chikusa-ku, Nagoya 464-8601, Japan.

*To whom correspondence should be addressed. E-mail: kimi@eri.u-tokyo.ac.jp

Fig. 1. (A) Bathymetry along the Japan Trench. The depth contour interval is 1000 m. An arrow indicates the plate convergence direction. A number of seamounts occur on the Pacific Plate offshore from the Ibaraki Prefecture (indicated as I). The dotted rectangle depicts the area shown in (B). (B) Seismic activity off Ibaraki, seismic profiles, and OBS stations (hexagons) of the surveys in 2004 (white), in 2005 (orange), and in 1998 and 2001 (magenta) (thin, reflection; thick, refraction). Circles show epicenters of $M > 3$ earthquakes in the Japan Meteorological Agency catalog (1996–2005), with focal depth scale at right and magnitude scale at bottom. A broken black line depicts the trench axis. A seismically quiet band (blue-shaded area) exists to the north of the source region of the 1982 M 7.0 event (green-shaded area; Fig. 2). A large yellow star marks its epicenter. Several furrows of different sizes are oriented in the direction of plate convergence (black arrows).



occurred on 7 May 2008 UTC). We modeled its rupture process by means of long-period teleseismic body waves (fig. S2). Its focal mechanism was a thrust type with the P axis in the subduction direction. The amount of slip appears to have been relatively small, averaging ~ 50 cm centered at ~ 25 km downdip from the hypocenter. However, an anomalously large rupture area raised its magnitude to 7.0. The local topographic bulge around its epicenter has been considered as evidence that an underlying subducted seamount defined the rupture area. The northern limit of the source region coincides with the edge of a ~ 25 -km-wide band of low seismic activity along the subduction direction (Fig. 1). Previous refraction (lines E and 11) and reflection (lines C and 11) sections through the seismically quiet band revealed low-velocity underthrust sediment layers with P -wave velocities (V_P) of ~ 4 km/s along the plate interface (16, 17). A trench-parallel reflection section (line C) beneath the seafloor furrows shows that the sediment layers are convex upward and have dimensions similar to those of the surrounding seamounts (fig. S6). Thus, the layer was interpreted as having formed in the wake of multiple subducted seamounts (16).

In 2004, we conducted an active-source seismic survey using ocean-bottom seismometers (OBSs) across the source region of the 1982 M 7.0 event along the trench-normal and trench-parallel profiles (Fig. 1). We derived two-dimensional V_P structures by P -wave first-arrival travel time inversion (Fig. 3). In contrast to the horizontally stratified structure to the north (fig. S4), the structure in and around the source region

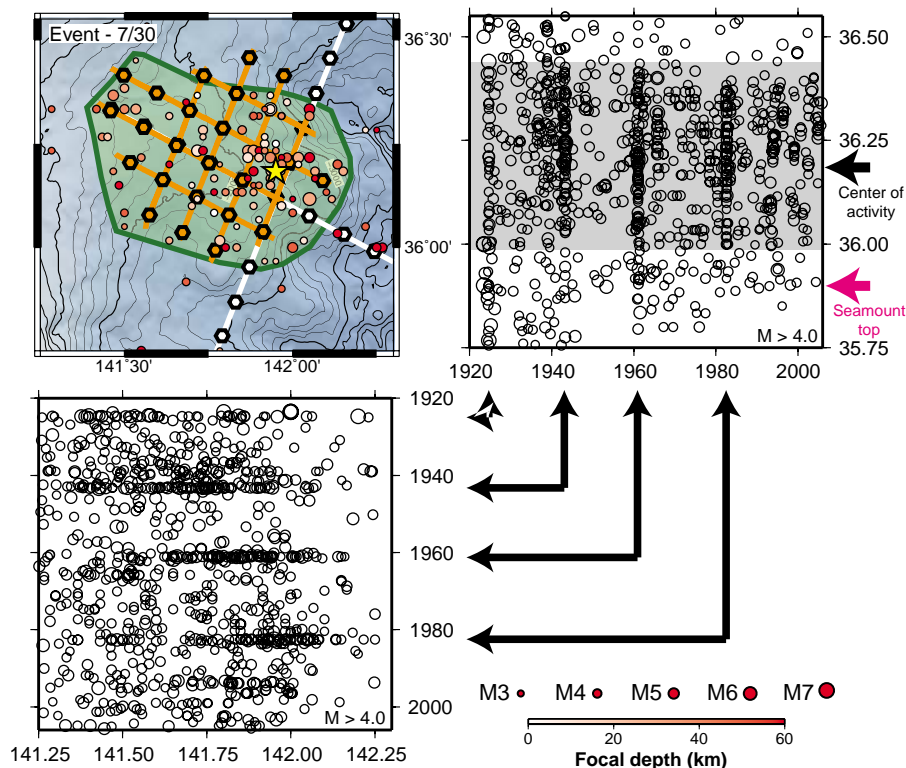


Fig. 2. Upper left: Aftershock activities of the 1982 M 7.0 earthquake. An estimated source region is indicated by the green-shaded area. Seismic profiles of the 2004 (white) and 2005 (orange) surveys and respective OBS stations are shown. Upper right and lower left: Chronological tables of earthquake activities in the region along the latitudinal and longitudinal axes. High earthquake activity associated with $M \sim 7$ earthquakes has occurred every ~ 20 years within a latitudinal band between 36.0°N and 36.4°N , centered at $\sim 36.2^\circ\text{N}$, substantially offset to the north from the subducted seamount (Fig. 4A).

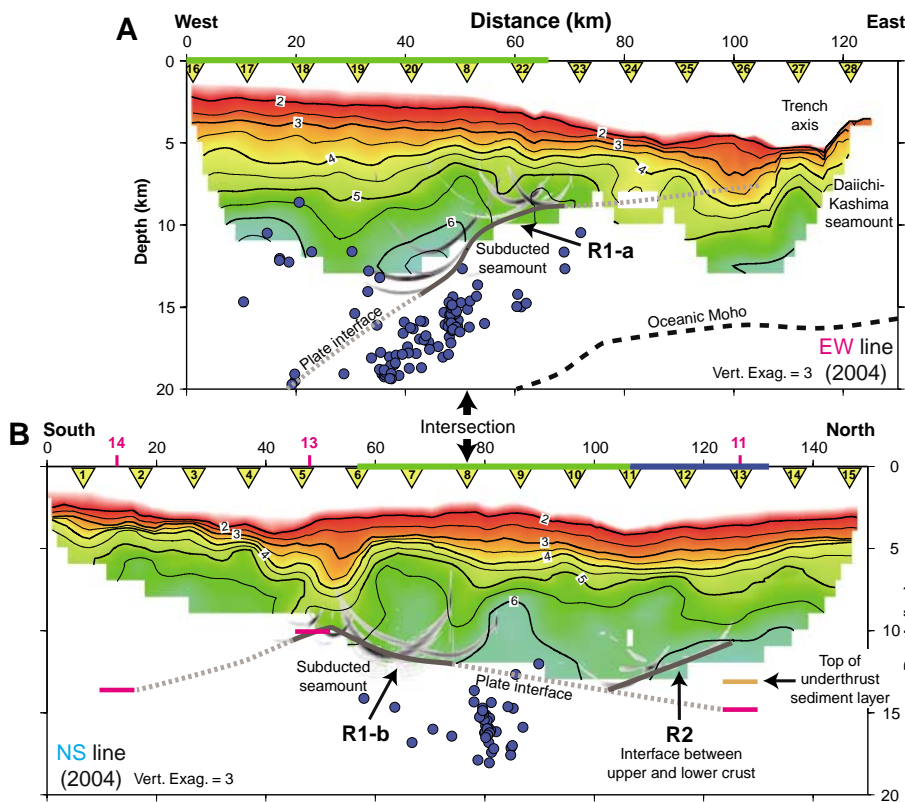


Fig. 3. (A) V_p structure along the trench-normal 2004 east-west (EW) line, and projected hypocenters observed during the 2005 seismic observation (within a 10-km-wide box on both sides along the profile for hypocenter projection). The OBS locations are shown by the yellow inverted triangles with their station numbers. A green bar along the top axis indicates the source region of the 1982 M 7.0 event. Geometry of the plate interface determined from strong reflections on the OBS record sections (hyperbolic black curves) outlines the convex upward structure (R1-a) interpreted as a subducted seamount. Earthquakes are concentrated beneath the subduction front of the seamount. (B) Same as (A) for the trench-parallel 2004 north-south (NS) line (hypocenters within a 7-km-wide box on both sides along the profile are projected). Depths to the plate interface (magenta bars) are determined on the trench-normal reflection sections (fig. S6). Corresponding line numbers of the sections are shown in magenta at the top axis. The depth to the top of the underthrust sediment is also shown (orange bar). The reflection interface in the north (R2) corresponds to the boundary between the upper and lower crust. A blue bar along the top axis indicates the seismically quiet band.

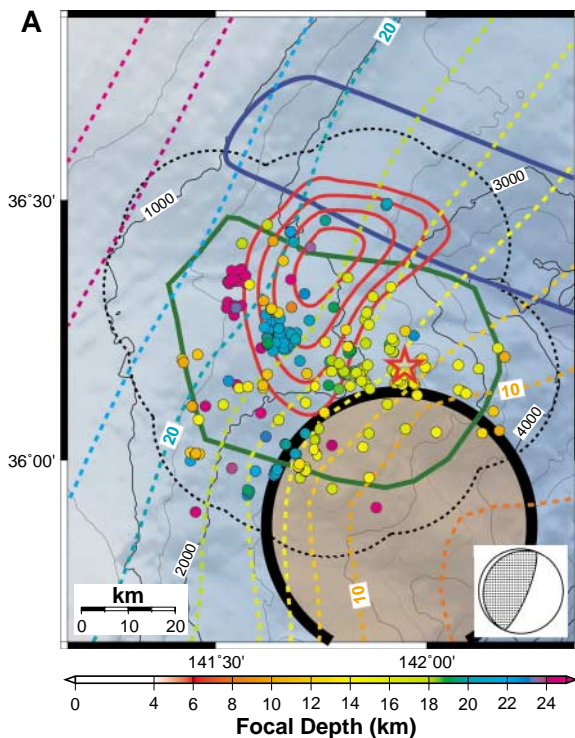


Fig. 4. (A) Geometry of the plate interface compiled from all available sections (dotted colored contours) and hypocenters of earthquakes observed during the 2005 seismic observation (depth scale at bottom). A red star indicates the epicenter of the 1982 event (its focal mechanism is shown at lower right). A thick black circle outlines the subducted seamount, a green curve denotes the source region of the 1982 event, and a blue curve shows a

seismically quiet band. Red contours indicate amounts of coseismic slip (outermost contour, 40 cm; interval, 10 cm). The dotted black curve surrounding the source region depicts an earthquake-search range by the OBS network. (B) Three-dimensional perspective view of the plate interface geometry. The hypocenter of the 1982 M 7.0 event is located at the base of the subducted seamount. It ruptured a region down dip.

shows a high degree of heterogeneity. Strong reflections on the OBS record sections (fig. S5) and projected reflection interfaces on the cross sections (Fig. 3) show two major structures at depths of 10 to 13 km: (i) a three-dimensional convex upward interface in the southeastern corner of the source region (R1), and (ii) a south-dipping interface in the seismically quiet band (R2).

The convex upward reflector (R1) outlines a part of the plate interface; its depth is the same as that of the plate interface traced from the trench on a reflection profile, line 13 (Fig. 3). By compiling the plate interface reflections on all existing cross sections, we constructed a three-dimensional geometry of the plate interface and mapped the subducted seamount (Fig. 4A). It has a basal diameter of ~50 km and a height of 3 km. Its size is comparable to that of the tallest seamount along the Japan Trench. Therefore, the 1982 *M* 7.0 event was located in front of the seamount (Fig. 4B).

The south-dipping reflector near the north end of the north-south line (R2) coincides with the along-dip seismically quiet band (Fig. 3B). Because our resolution was too low beneath the interface, we performed a qualitative test of reflection amplitudes with varying *P*-wave velocity contrasts across the interface (fig. S5C). The results imply that the reflector represents part of the interface between the upper and lower crust of the overriding plate. The horizontal structure to the north beneath the flat seafloor without furrows, away from any subducted seamount, agrees with this interpretation (fig. S4). The observed underthrust sediment layer lies beneath this south-dipping interface (Fig. 3B). Therefore, it appears that subduction of multiple seamounts has had an impact on the base of the overriding plate, possibly eroding it.

To characterize the microearthquake activity and its relation with the seamount, we conducted a 1-month-long passive seismic observation over the source region in 2005 (fig. S7) and recorded 257 precisely determined hypocenters. Earthquakes were concentrated at the base of the subducted seamount along the down-dip edge and its associated ridge (Figs. 3 and 4A). Seismicity was confirmed to be low in the quiet band.

No earthquakes occurred over the subducted seamount during our recording period (Figs. 3 and 4A). The lack may be explained by either very weak or nearly perfect interplate coupling. We favor the first explanation because the 1982 event was initiated from its hypocenter at the base of the seamount and ruptured down-dip (Fig. 4B), and because the series of repeating large earthquakes also appear to have occurred next to the seamount (Fig. 2).

We propose that friction is low along the plate interface both over the subducted seamount and in the wake of its subduction (Fig. 4B). Our results suggest that a subducted seamount may concentrate stress at its subduction front where large earthquakes with a broad rupture area can be initiated. The width of the seamount may influence the area of rupture. The seismic coupling within this region appears to be relatively weak, as an average slip of ~50 cm accounts for only ~30% of the amount of plate convergence during the 20-year interseismic period. Fluid migration may further determine the coupling along the plate interface around the base of the seamount. Fluid-rich sediment entrained with the seamount may produce a weakly coupled zone in its wake. Seismic ruptures, therefore, can be blocked both at the seamount and in the wake.

References And Notes

1. J. Kelleher, W. McCann, *J. Geophys. Res.* **81**, 4885 (1976).
2. M. Cloos, *Geology* **20**, 601 (1992).
3. J. K. Hillier, A. B. Watts, *Geophys. Res. Lett.* **34**, 10.1029/2007GL029874 (2007).
4. C. H. Scholz, C. Small, *Geology* **25**, 487 (1997).
5. S. Bilek, S. Y. Schwartz, H. R. DeShon, *Geology* **31**, 455 (2003).
6. S. Husen, E. Kissling, R. Quintero, *Geophys. Res. Lett.* **29**, 10.1029/2001GL014045 (2002).
7. S. Kodaira, N. Takahashi, A. Nakanishi, S. Miura, Y. Kaneda, *Science* **289**, 104 (2000).
8. C. R. Ranero, R. von Huene, *Nature* **404**, 748 (2000).
9. N. L. B. Bangs, S. P. S. Gulick, T. H. Shipley, *Geology* **34**, 701 (2006).
10. S. Dominguez, J. Malavieille, S. E. Lallemand, *Tectonics* **19**, 182 (2000).
11. P. R. Cummins, T. Baba, S. Kodaira, Y. Kaneda, *Phys. Earth Planet. Inter.* **132**, 75 (2002).
12. R. von Huene, C. R. Ranero, P. Vannucchi, *Geology* **32**, 913 (2004).
13. C. DeMets, R. G. Gordon, D. F. Argus, S. Stein, *Geophys. Res. Lett.* **21**, 2191 (1994).
14. S. Lallemand, R. Culotta, R. von Huene, *Tectonophysics* **160**, 231 (1989).
15. Dominguez *et al.*, *Tectonophysics* **293**, 207 (1998).
16. T. Tsuru *et al.*, *J. Geophys. Res.* **107**, 10.1029/2001JB001664 (2002).
17. S. Miura *et al.*, *Tectonophysics* **363**, 79 (2003).
18. We thank S. Hashimoto and T. Yagi for their assistance through preparation and operations of the OBSs; the captain and crew members of *RV Hakuho-Maru* for their efforts to carry out the surveys and observation; T. Tsuru for discussion and providing us with published reflection sections; N. L. B. Bangs, N. Hirata, G. F. Moore, S. Okubo, and H. Sato for reviews; and Y. Fukao for discussion. Supported by the Ministry of Education, Culture, Sports, Science and Technology of Japan.

Supporting Online Material

www.sciencemag.org/cgi/content/full/321/5893/1194/DC1

Materials and Methods

Figs. S1 to S9

References

9 May 2008; accepted 10 July 2008

10.1126/science.1160250

Limits for Combustion in Low O₂ Redefine Paleatmospheric Predictions for the Mesozoic

C. M. Belcher* and J. C. McElwain

Several studies have attempted to determine the lower limit of atmospheric oxygen under which combustion can occur; however, none have been conducted within a fully controlled and realistic atmospheric environment. We performed experimental burns (using pine wood, moss, matches, paper, and a candle) at 20°C in O₂ concentrations ranging from 9 to 21% and at ambient and high CO₂ (2000 parts per million) in a controlled environment room, which was equipped with a thermal imaging system and full atmospheric, temperature, and humidity control. Our data reveal that the lower O₂ limit for combustion should be increased from 12 to 15%. These results, coupled with a record of Mesozoic paleowildfires, are incompatible with the prediction of prolonged intervals of low atmospheric O₂ levels (10 to 12%) in the Mesozoic.

Atmospheric O₂ has played a key role in the development of life on Earth, with the rise of O₂ in the Precambrian being closely linked to biological evolution (1). Vari-

ations in the concentration of atmospheric O₂ throughout the Phanerozoic are predicted from models based on geochemical cycling of carbon and sulfur (2, 3). Such models predict atmospher-

ic O₂ concentrations as low as 10% (3) or 12% (2) (present atmospheric O₂ is 20.9%) in the Mesozoic [251 to 65 million years ago (Ma)], and low (<12%) O₂ atmospheres are hypothesized to be the primary driver of at least two of the “big five” mass-extinction events in the Phanerozoic (1, 4). Few proxies have been developed for testing models of past atmospheric O₂ concentrations, particularly the low O₂ levels predicted for the Permo-Triassic boundary (3) and throughout the Triassic (3) and Jurassic (2). The presence of charcoal in the geological record provides one means to test predicted paleoatmospheric O₂ levels (5). Several studies have sought to test the limits of combustion under varying concentrations of O₂ (6–8); early work observed that the minimum O₂ level required for the combustion of CO and CH₄ was 13% (6) and that paper would burn at 15% O₂ (7). More recent work found that dry (0 to 2%

School of Biology and Environmental Science, University College Dublin (UCD), Belfield, Dublin 4, Ireland.

*To whom correspondence should be addressed. E-mail: claire.belcher@ucd.ie